*Romanian Reports in Physics, Vol. 64, No. 3, P. 891–904, 2012*

# A NEW POSSIBILITY OF EXPERIMENTAL CHARACTERIZATION OF A TIME OF FLIGHT TELEMETRIC SYSTEM

ANDREEA RODICA STERIAN[1], OCTAVIA BORCAN[2], CATALIN SPULBER[2], PAUL STERIAN[1] , FLORIN TOMA[2]

[1] "Politehnica" University of Bucharest, Physics Department, 313 Splaiul Independentei St., Bucharest 060042, Romania, E-mail: andreea.sterian1@yahoo.com
[2] PROOPTICA SA, 67 Gh.Petrascu St., Bucharest, 031593, Romania, E-mail: borcan_octavia@yahoo.com, catalin.spulber@yahoo.com

*Received July 25, 2011*

*Abstract.* The purpose of this paper is to assess the rangefinder probability in different weather visibilities. The authors show that the rangefinder distance can be simulated in lab conditions, by using a rangefinder equipment, a photosensitive plate and some neutral filters with known absorption. The results obtained in lab conditions were compared with field measurements and the differences were not significant. Interpretation of results was based on the Bayes' theorem, taking into account that the visibility of seen objects is depending by the subjectivity of human observation, laser beam positioning errors on the objects and the emission power limited by atmospheric condition.

*Key words*: rangefinder equipment, simulation, atmospheric transmission, optical filters, rangefinder distance.

## 1. INTRODUCTION

The studied based on an erbium laser ($\lambda = 1.54$ μm) telemeter (produced by SC PRO OPTICA SA, Romania) measures the time of flight of an optical pulse going to the target at distance $L$ and back, in different working conditions determined by the particular application [1, 10]. The precision of the device is ± 10 m. As well as the uncertainity $\Delta T$ of the measurements reflects itself in a distance uncertainity $\Delta T = c\Delta T/2$, we require that the pulse duration $\tau$ to be short enough for the desired resolution, that is $\tau = \Delta T$.

To characterize such a kind of system we must evaluate first its power budget taking into account the attenuation due to geometrical effects, the additional contribution from the transmittance $\tau_{opt}$ of the transmitter/receiver lenses and from the attenuation coefficient of the air [2, 3] in the equation:

$$\tau_{atm} \approx \exp[-2\alpha L], \tag{1}$$

where $\alpha = \alpha(\lambda)$, $\lambda$ being the optical wavelength.
We have the equation:

$$\frac{P_r}{P_s} = \frac{GD_r^2}{4L_{eq}^2} \tag{2}$$

where $P_s$ is the power of the optical source, $P_r$ is the received power, $L_{eq}$ is the equivalent distance, $L_{eq} = L/\tau_{atm}$, $D_r$ is the receiver objective lens diameter and $G$ is a gain factor given by $G = \tau_{opt}\cdot\delta$ for a no-cooperative target and $G = \tau_{opt}/\theta_s^2$ for a cooperative target, $\delta$ being a fraction power re-diffused back to the receiver by the target and $\theta_s$ the angular divergence of the optical source [1, 4].

If $P_n$ is the noise power of the receiver circuit, by the requirement that the ratio:

$$\frac{S}{N} = \frac{P_r}{P_n} \tag{3}$$

to be higher that ten for a good measurement, we get finally the system equation of the telemeter:

$$GP_s = \left(\frac{S}{N}\right) P_n \frac{4L_{eq}^2}{D_r^2}, \tag{4}$$

which relates the required $S/N$ ratio to the receiver noise $P_n$ and to attenuation $4\cdot L_{eq}^2/D_r^2$.

Power emission – reception ratio give indications on the measured distance $R$, but by real determinations and simulation as well, one can estimate and quantify other important factors that influence the measured distance $R$: the objective diameter of the emission source $D_{ob}$, atmospheric transmission $\tau$, the object reflectivity $\rho$, the signal noise ratio $S/N$ (Figs. 1–4, below):

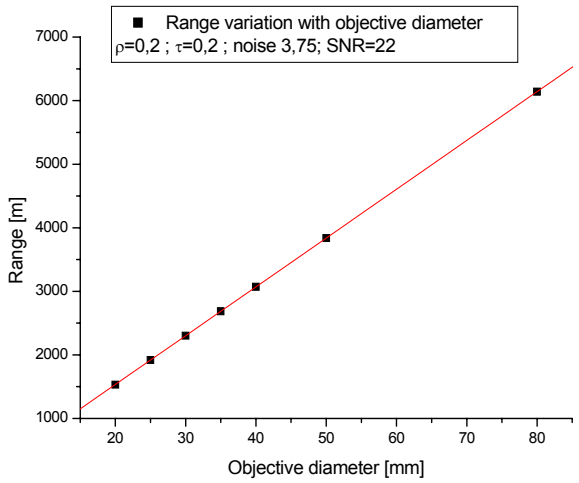


Fig. 1 – The rangefinder distance variation with objective diameter; $R_{max} = R_{max}(D_{ob})$.

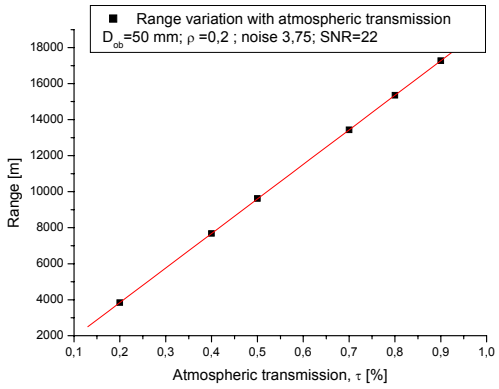


Fig. 2 – The rangefinder distance variation with atmospheric transmission; $R_{max} = R_{max}(\tau_{atm})$.

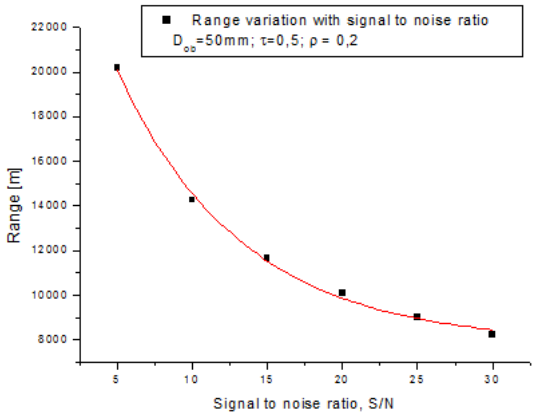


Fig. 3 – The rangefinder distance variation with signal to noise ratio; $R_{max} = R_{max}(S/N)$.

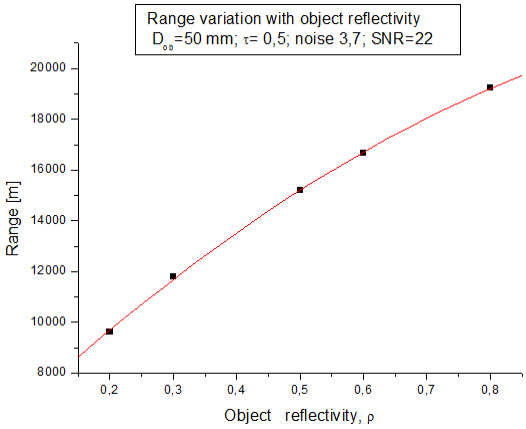


Fig. 4 – The rangefinder distance variation with object reflectivity; $R_{max} = R_{max}$ (rediffused power δ).

On the basis of Bayes theorem, by connections between real results in field, in different atmospheric transparencies and data obtained in laboratory experiments, the authors propose a relationship for range measurement probability, in the case of a given target. This relationship takes into account the attenuation coefficient σ (Fig. 5) and the received signal power, $P_r$, which is known to be of the form:

$$P_r = P_s \cdot \tau_{\text{atm}}, \tag{5}$$

and is in direct relation with the laser diameter measured at its emission and at its reception and also with the calculated contrast in the acquired images.

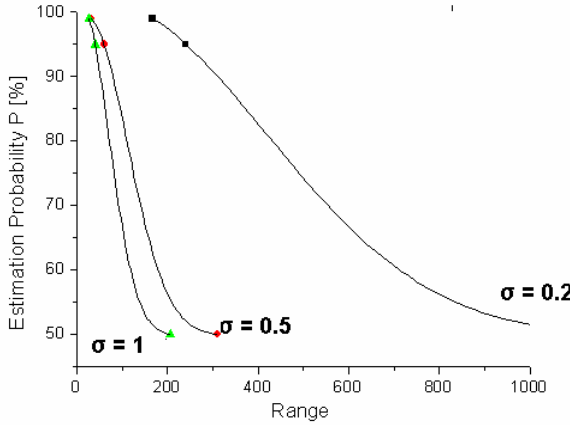


Fig. 5 – Range measurement probability estimated from the atmospheric transmission, expressed here by the attenuation coefficient σ [5].

## 2. EXPERIMENTAL METHODOLOGY

The main characteristics of the flight telemeter system are: the wavelength λ = 1.54 μm, the output power is $P_e$ = 0.18W and the divergence of the beam is 0.6 mrad. Lab tests regarding the performance characteristics as diameter's laser beam at emission and reception can be highlighted by the setup bellow (Fig. 6).

An alternative at the setup showed in Fig. 6 is the use of a lens placed near the laser source to amplify its power and see more clear the traces of the laser beam. The photosensitive plate is then placed in the focal plane of the lens ($f_{ob}$ =342 mm). Four attenuation neutral filters with 30%, 35%, 52 % and 75% transmissions were placed in the front of the plate, one by one, to simulate the atmospheric transmission variation on the lab stand (Fig. 7). The difference between the diameter holes, or even more, between its areas, due to emission and that ones due to reception, shows the difference between power emission and reception [6].

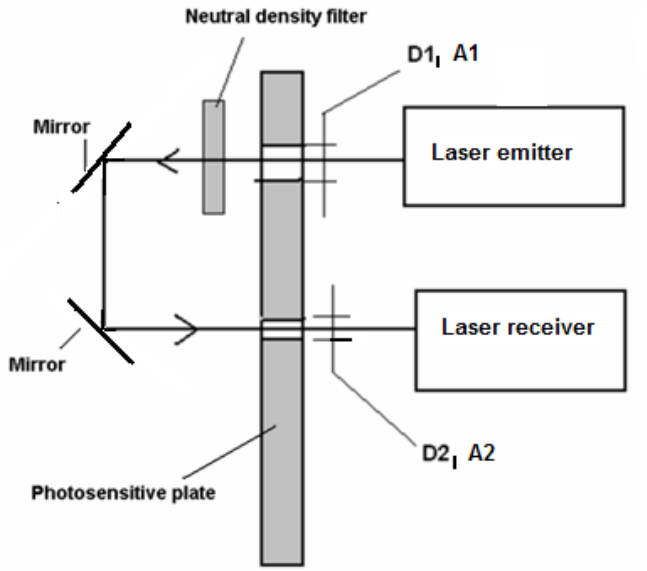


Fig. 6 – The scheme used to measure the powers ratio by measuring the areas $A_1$ and $A_2$ or diameters $D_1$ and $D_2$.

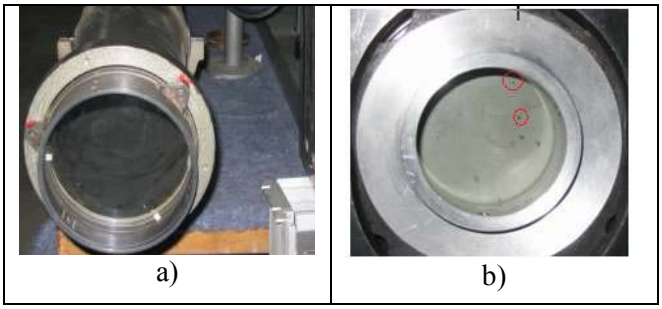


Fig. 7 – General view of the photosensitive plate, before (a) and after (b) the impact with the laser beam; several contact points impressed on the photosensitive plate are obtained.

Real measurements of some targets, in different atmospheric transparency were made too (Figs. 8, 9, 10, 11). One can make then a software analysis of the images to obtain a correlation between measured diameter or area of the laser beams and the contrast variation in image (which is proportional with the atmospheric transmission variation). These data can be used later to simulate the measured performances that can be obtained with a rangefinder with given constructive parameters, in known atmospheric conditions.

The measured targets (1–7) were buildings located at different known distances, as follows: 1–150 m; 2–249 m; 3–205 m; 4–280 m; 5–363 m; 6–1498 m; 7–2590 m (Figs. 8–11). The distances have been obtained from official topographic data.

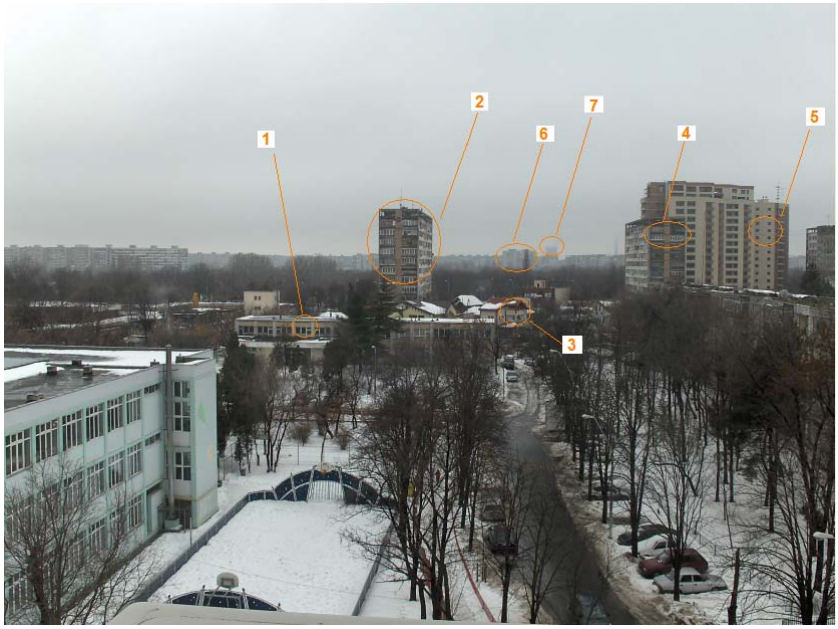


Fig. 8 – Example of an image acquired in normal atmospheric transparency for a winter day (visibility is 4,5 km); target 7 was the last possible rangefinder measured distance.

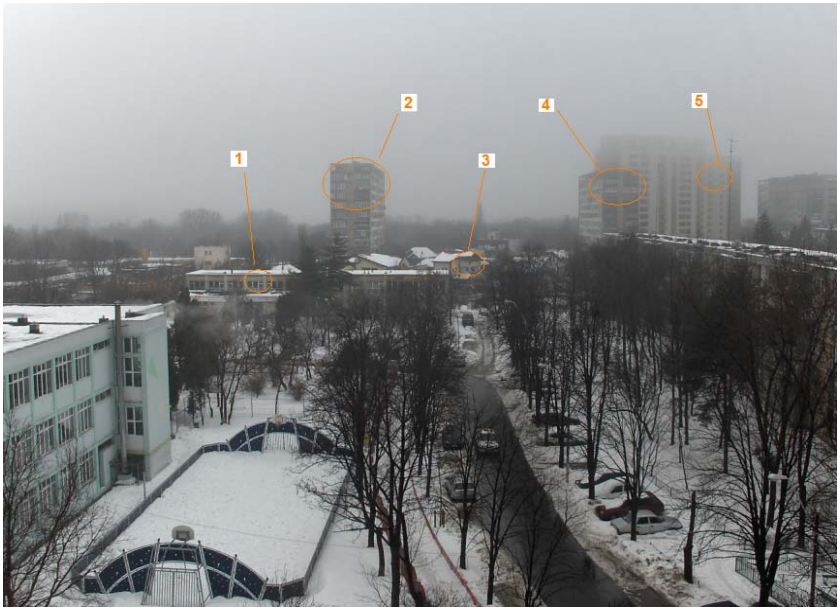


Fig. 9 – Example of an image scene acquired in lower atmospheric transparency (visibility is 1,4 km); target 5 was the last possible rangefinder measured distance.

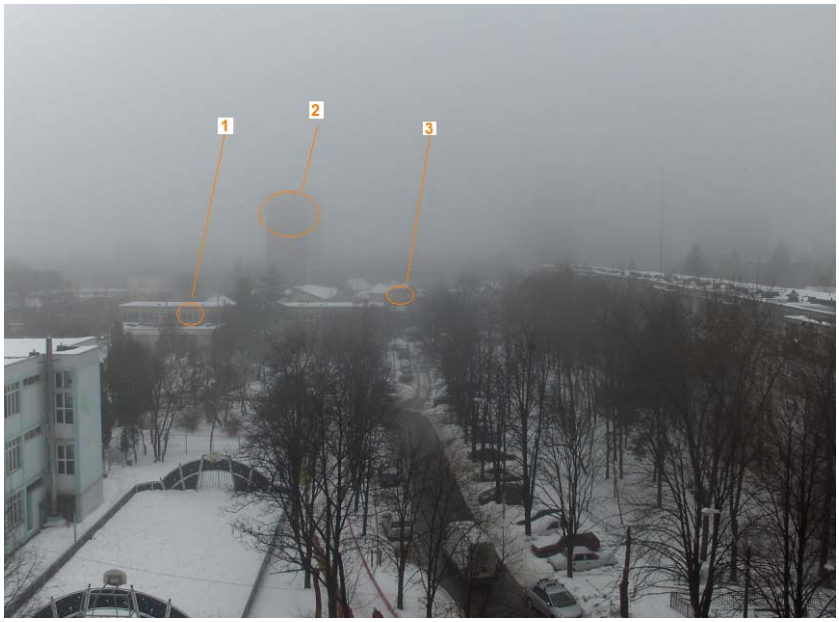


Fig. 10 – Image scene acquired in lower atmospheric transparency (visibility is 500 m); target 3 was the last possible rangefinder measured distance.

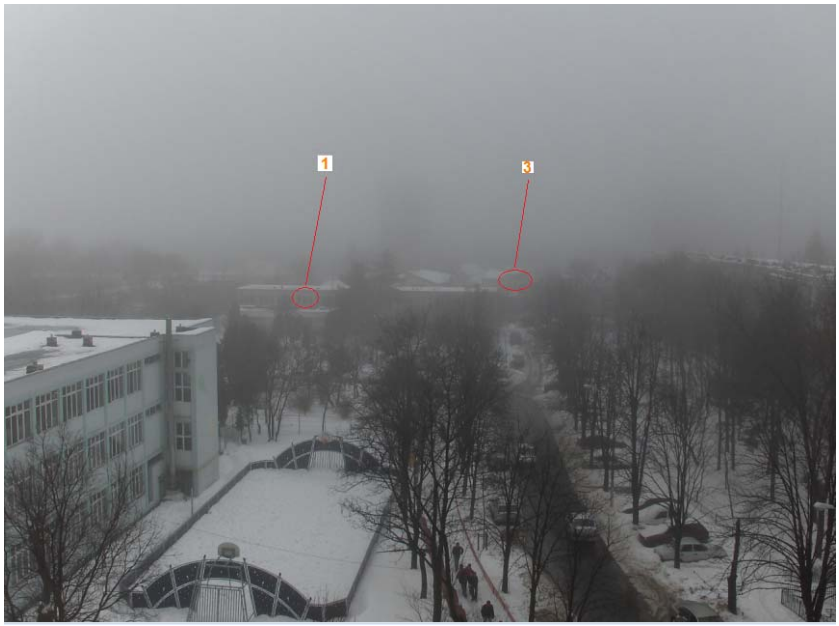


Fig. 11 – Example of the same image scene acquired in a much lower atmospheric transparency (visibility is 350 m); target 3 was the last possible rangefinder measured distance.

## 3. RESULTS

As result of the five laser beam shootings on the photosensitive plate, five holes were obtained, with different areas, smaller as the filter absorption was higher at the laser wavelength (Fig.12).

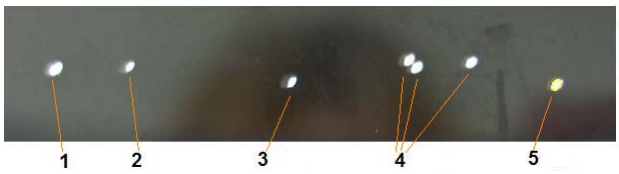


Fig. 12 - The image of the laser beam areas on the photosensitive plate when the surface is placed in the focal plane of the lens; the holes are as follows: 1 – without filter; 2 – with a filter of 30% transmission; 3 – with 35% transmission; 4 – with 52% transmission; 5 – with 75% transmission.

If the photosensitive plate is placed at a higher distance than the objective focal length, partial holes are obtained, at different contrasts $C_R$ (Fig. 13).

The contrast $C_R$ is the threshold contrast get by the laser beam which yet allows the rangefinder process.

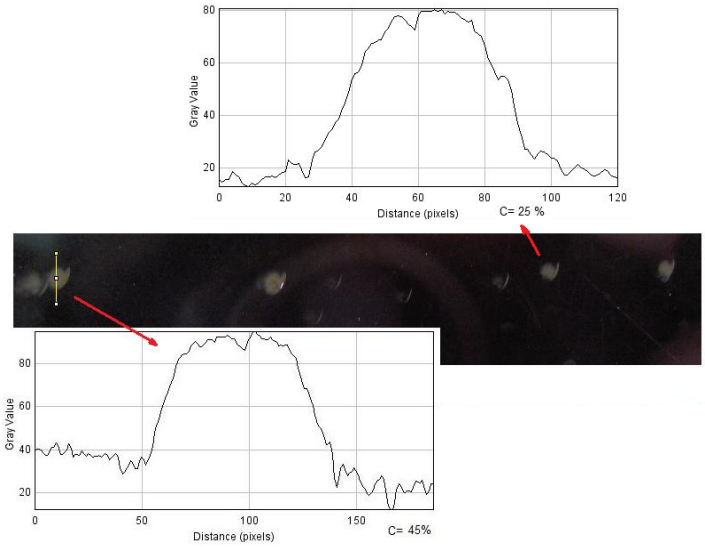


Fig. 13 – The image of the laser beam areas on the photosensitive plate when this surface is placed at a higher distance than the objective focal length; two contrast variation diagrams are given here as example.

The results obtained and showed in Figs. 12–13 can be transposed in the diagram bellow (Fig. 14).

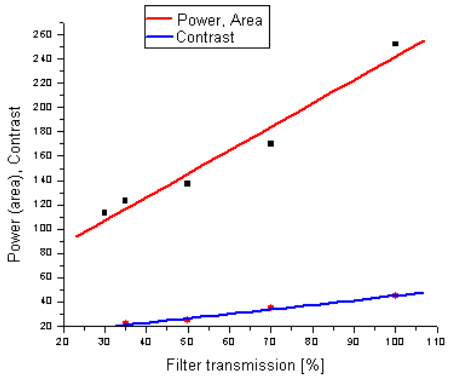


Fig. 14 – As the filter transmission is increasing, the power received is increasing too.

Relationships by the form expressed bellow can be extracted from Fig. 14:

$$\frac{P}{P_0} = 49 + 1.9 \cdot \tau \qquad \text{or} \qquad \frac{P}{P_0} = 7 + 5.1 \cdot C_R . \tag{6}$$

One can therefore say that the rangefinder probability depends by the value ratio of emission and reception powers $P_e$ / $P_r$.

In other words, as the ratio of the laser beams areas $A_2$ / $A_1$ on the photosensitive plate is increasing, the rangefinder probability is increasing too. Therefore, one can make the statement that the rangefinder probability can be expressed as a relation by the following form:

$$P_{telem}(\tau) = \text{const.} \frac{A_2}{A_1} . \tag{7}$$

For a rangefinder with given technical features (§ 2), the rangefinder probability has the shape presented in Fig. 15, in normal visibility conditions.

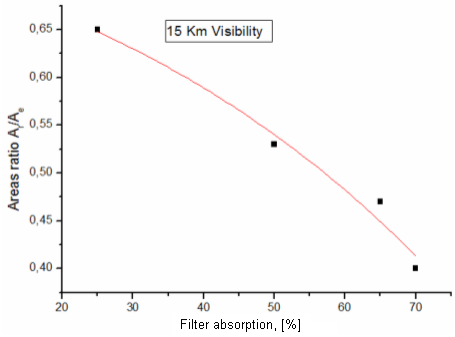


Fig. 15 – The areas ratio $A_2$ / $A_1$ can estimate the rangefinder probability in normal visibility conditions.

On the other hand, by analyzing the scene images acquired during the rangefinder process, one can noted that the rangefinder distances depends by the atmospheric visibility and implicitly by the image contrast between the target and the background. One can calculate it by an image analyzing software.

With the real measured distances in the field, one can draw the diagram of the rangefinder distances depending by visibility, for an about extinction coefficient $\sigma = 0.6 \times 10^{-3}$.

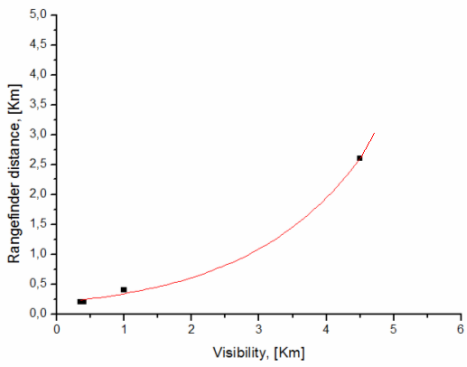


Fig. 16 – The rangefinder distance variation with visibility, in poor and medium atmospheric transmission.

The relationship between measured distance and visibility is by the following form:

$$R=0.2\cdot e^{V/1.7}\ [\text{km}]. \tag{8}$$

Using this relationship, one can noted that, for this given rangefinder used in these experiments, the limit of correct using is about 5.5 km when the atmospheric visibility is 3…4 times lower than the normal one.

If the visibility is much lower, towards few hundreds of meters, the rangefinder probability is dramatically decreasing, as one can see in Fig. 17.

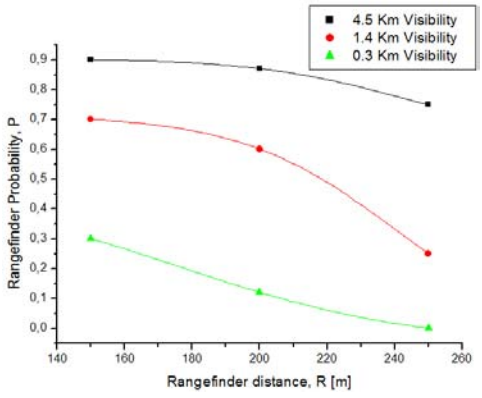


Fig. 17 – Rangefinder probability depends by the measured distance and the visibility conditions.

For calculating the rangefinder probability in the field, an admissible measurement error of about ±10 m was considered around the known value of target's distance. The relationship used was as following form:

$$P = n/N \tag{9}$$

where $n$ is the number of correct measured distances and $N$ is the number of total attempts.

The measurements were made for different targets in different visibility conditions.

The diagram of the rangefinder probability is done by a Boltzmann function:

$$P = \frac{k_1}{1 + e^{\frac{R-k_2}{k_3}}} + k_4 . \tag{10}$$

Its shape is similar with that one obtained in lab conditions and a correlation between them can be made (Fig. 18).

Another possibility to express the rangefinder probability, depending by visibility, is shown in Fig. 19.

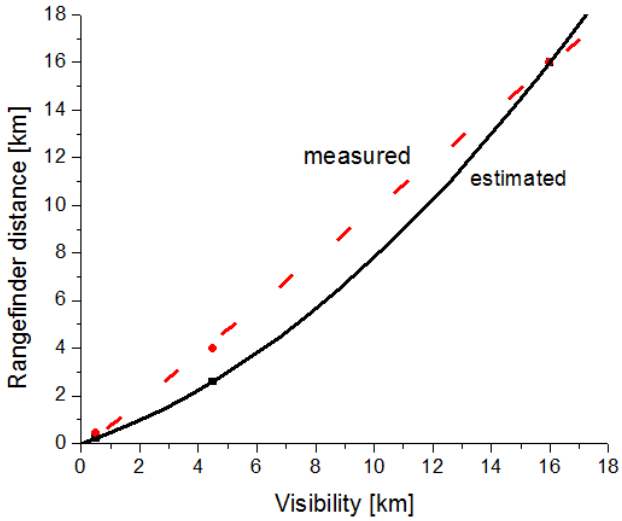


Fig. 18 – A correlation between the measured rangefinder distance and the estimated one in lab conditions can be made.

Practically we can't speak about a rangefinder determination without observing the target. A relationship to estimate the rangefinder probability, but conditioning it with the observation probability can be done starting from the Bayes's theorem.

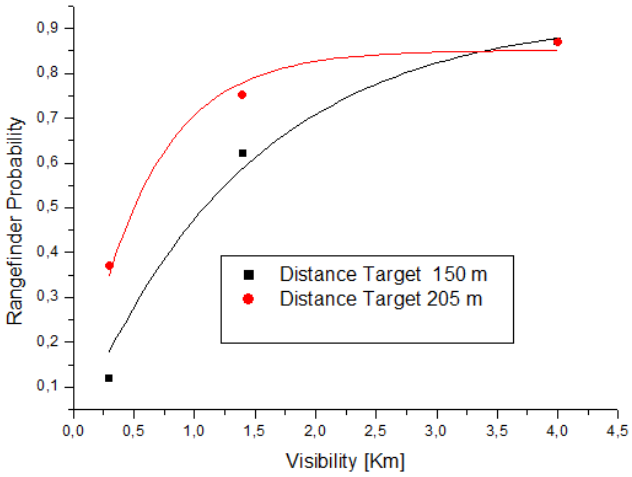


Fig. 19 – For different target distances, rangefinder probabilities may be different even for the same visibility.

Bayes's theorem is of the following form [7]:

$$P(x|y) = \frac{P(y|x) \cdot P(x)}{P(y)}, \tag{11}$$

where $P(x|y)$ is the probability to rangefinder a target when one sees it (a rangefinder process conditioned by observation); $P(y|x)$ is the probability to see the target when one range finds it (an observation process conditioned by rangefinder); this probability can be practically interesting for a rangefinder process in low light level, using a simple CCD (charge-coupled device) camera; $P(x)$ is the rangefinder probability, which depends mainly by the laser power; $P(y)$ is the observation probability which depends mainly by the atmospheric transmission, some optical features of the equipment and the operator's age and experience.

The Ideal case is when atmospheric transmission is good, light level is optimal, the equipments are performing, the operator is trained.

## 4. DISCUSSION

There is a certain level of visibility until one can measure a certain distance; then, even if the target is still visible, the rangefinder process is not more possible.

The rangefinder distance $R$ tends toward visibility distance, $V$, but $R \neq V$. This means that:

1) For a very good visibility: $P(x|y) \approx P(y|x)$;

2) For a middle visibility: $P(x|y) < P(y|x)$.

The probability to observe well a target if one measure correctly a distance to it with the rangefinder is bigger than the probability to measure correctly a distance to the target if one can see the target well (because of the errors induced by the atmospheric absorption, incorrect positioning of the rangefinder, lack of training, etc.). Obviously, one can consider $P(y \mid x) = 1$ in a middle visibility at a day light level.

3) For a poor visibility: $P(x \mid y) = P(y \mid x)$.

Interesting for study is the second case. In conclusion, in the case of a middle visibility and day light level, $P(y) > P(x)$ and one can consider the following relationship:

$$P(x|y) = \frac{P(x)}{P(y)}. \tag{12}$$

The observation probability, $P(y)$ or $P_{obs}$ with a CCD camera, can be experimentally expressed by correlation with the target's image contrast and the light level [8, 9]. The Bayes theorem can be also applied here.

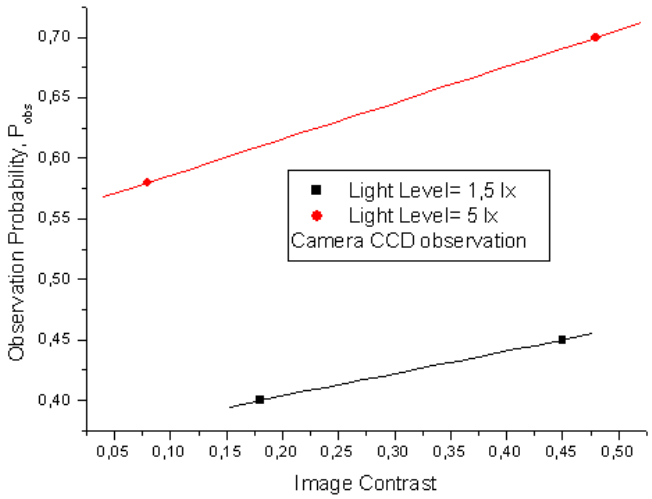


Fig. 20 – The observation probability is increasing with the image contrast of the target and with the light level.

A relationship for the rangefinder determination conditioned by observation can be expressed as follows:

$$P(x|y) = \frac{\text{const.} \times A_1 / A_2}{P_{obs}}. \tag{13}$$

## 5. CONCLUSIONS

1. It is possible to use a synthetic and simple experimental simulation method to estimate the rangefinder distance and the measured contrast of the image acquired, even without knowing the ambient conditions, if the approximate target's size and reflectivity are previously known;

2. Relationships between the measured distance in field, the required rangefinder probability, the atmospheric nebulosity's degree and the variable visual contrast between target and background can be obtained;

3. Valid decisions can be made in situations that impose a quick intervention, by an algorithm based on the proposed relationships.

4. The most common situations occur when the visibility is at a medium value and the rangefinder measurements are during the day. In this case, a relationship to estimate the rangefinder probability in relation with the observation probability can be done starting from the Bayes's theorem.

5. It's frequently happens to see the target well enough but the measured value not being correct. If the transparence atmosphere value is low, rangefinder errors can appear and their values must be known.

## REFERENCES

1. Y. Reshetyuk, *Investigation and calibration of pulsed time-of-flight terrestrial laser scanners*, Stockholm, Royal Institute of Technology, Licentiate thesis in Geodesy, October 2006.
2. R. Sabatini, *Tactical laser systems performance analysis in various weather conditions*, In Meteorological Conditions Considering Out-of-Area Operations", Italian Air Force Academy, Naples, Italy, 16-19 March, 1998, pp.29-1-29-13.
3. S. Donati, *Electro-Optical Instrumentation: Sensing and Measuring with Lasers*, Prentice Hall, 2004, pp. 39–71.
4. Y. Fumin, H. Peicheng, C. Wanzhen, Z. Zhongping, C. Juping et al., *Progress on Laser Time Transfer Project*, 15th International Workshop on Laser Ranging, Canberra, Australia, 15–20 October, 2006.
5. G.C. Holst, *Electro-Optical Imaging System Performance*, SPIE Optical Engineering Press, JCD Publishing, Winter Park, FL., 1995.
6. F. Blais, J.A. Beraldin, S.El- Hakim, *Range Error Analysis of an Integrated Time-of-Flight, Triangulation, and Photogrammetric 3D Laser Scanning System, Laser Radar Technology and Applications V*, Proceedings of SPIE's Aerosense 2000, Vol. 4035, pp.236-247, 24-28 April 2000, Orlando, FL.
7. W. Burgard, *Recursive Bayes Filtering*, *Advanced AI*, www.informatik.uni-freiburg.de/~ki/teaching/ws0607/advanced/recordings/BayesFiltering.ppt
8. O. Borcan, C. Spulber, *Contributions to the evaluation of observability performance in difficult ambient conditions, for observation equipment during night and day*, Proc. SPIE, Electro-Optical Remote Sensing, Photonic Technologies, and Applications III , 7482, pp. 74820V-74820V-12, Society of Photo-Optical Instrumentation Engineers, Bellingham, WA, ETATS-UNIS, 2009.
9. O. Borcan, C. Spulber, *Experimental method for observation prediction based on the decision matrix, through day/ night equipments in NIR and LWIR spectral ranges*, Proc. of SPIE, Infrared Imaging Systems: Design, Analysis, Modeling, and Testing XX, 7300, pp. 730011-1, Society of Photo-Optical Instrumentation Engineers, Bellingham, WA, ETATS-UNIS, 2009.
10. Andreea Rodica Sterian, *Coherent Radiation Generation and Amplification in Erbium Doped Systems* (Ch. 12), in *Advanced in Optica Amplifiers* by Paul Urquart (Editor), published by InTcch, Vienna, 2001, p. 255.